THE JOURNAL OF BIOLOGICAL CHEMISTRY VOL. 289, NO. 25, pp. 17680–17688, June 20, 2014

A Novel Ste20-related Proline/Alanine-rich Kinase (SPAK)-independent Pathway Involving Calcium-binding Protein 39 (Cab39) and Serine Threonine Kinase with No Lysine Member 4 (WNK4) in the Activation of Na-K-Cl Cotransporters*

Received for publication, December 4, 2013, and in revised form, April 7, 2014 Published, JBC Papers in Press, May 8, 2014, DOI 10.1074/jbc.M113.540518

Jose Ponce-Coria[‡], Nicolas Markadieu[‡], Thomas M. Austin[‡1], Lindsey Flammang[‡], Kerri Rios[‡], Paul A. Welling[§], and Eric Delpire[‡2]

From the [‡]Department of Anesthesiology, Vanderbilt University School of Medicine, Nashville, Tennessee 37232 and the [§]Department of Physiology, University of Maryland School of Medicine, Baltimore, Maryland 21201

Background: WNK4 acts upstream of SPAK/OSR1 in the regulation of Na-K-2Cl cotransporters.
Results: Here we show that WNK4 directly binds to NKCC1, and in the presence of Cab39 it stimulates NKCC1 activity.
Conclusion: WNK4 regulates NKCC1 through SPAK/OSR1-dependent and SPAK/OSR1-independent pathways.
Significance: We uncovered a novel mode of Na-K-2Cl cotransporter activation which involves a direct interaction of WNK4 with the cation-chloride cotransporter.

Na^+-dependent chloride cotransporters (NKCC1, NKCC2, and NCC) are activated by phosphorylation to play critical roles in diverse physiological responses, including renal salt balance, hearing, epithelial fluid secretion, and volume regulation. Serine threonine kinase WNK4 (With No K = lysine member 4) and members of the Ste20 kinase family, namely SPAK and OSR1 (Ste20-related proline/alanine-rich kinase, Oxidative stress-responsive kinase) govern phosphorylation. According to present understanding, WNK4 phosphorylates key residues within SPAK/OSR1 leading to kinase activation, allowing SPAK/OSR1 to bind to and phosphorylate NKCC1, NKCC2, and NCC. Recently, the calcium-binding protein 39 (Cab39) has emerged as a binding partner and enhancer of SPAK/OSR1 activity, facilitating kinase autoactivation and promoting phosphorylation of the cotransporters. In the present study, we provide evidence showing that Cab39 differentially interacts with WNK4 and SPAK/OSR1 to switch the classic two kinase cascade into a signal kinase transduction mechanism. We found that WNK4 in association with Cab39 activates NKCC1 in a SPAK/OSR1-independent manner. We discovered that WNK4 possesses a domain that bears close resemblance to the SPAK/OSR1 C-terminal CCT/PF2 domain, which is required for physical interaction between the Ste20 kinases and the Na^+-driven chloride cotransporters. Modeling, yeast two-hybrid, and functional data reveal that this PF2-like domain located downstream of the catalytic domain in WNK4 promotes the direct interaction between the kinase and NKCC1. We conclude that in addition to SPAK and OSR1, WNK4 is able to anchor itself to the N-terminal domain of NKCC1 and to promote cotransporter activation.

Function of the Na-K-2Cl cotransporter, NKCC1,[3] is critical to many physiological systems. Located on the basolateral membrane of a variety of epithelia, NKCC1 participates to the trans-cellular movement of ions. For instance, in salivary, lacrimal, sweat, lung, pancreas, and intestinal epithelia, the cotransporter replenishes cellular Cl^- as the anion is transported across the apical membrane (*e.g.* through cystic fibrosis transmembrane conductance regulator Cl^- channels). Thus, in these epithelial tissues, NKCC1 participates in secretion of fluid and Cl^-. In contrast, in the stria vascularis, a stratified epithelium of the inner ear, the cotransporter replenishes cellular K^+ as the cation is transported across the apical membrane through the Kv7.1 (KvLQT1) potassium channel. Disruption of NKCC1 in mice results in phenotypes associated with fluid disruption in many of these epithelia (1), including the most striking phenotype which derives from a deficit in secretion of the K^+-rich endolymphatic fluid, leading to imbalance and sensorineural deafness (2, 3). NKCC1 is also involved in the control and maintenance of cell volume as well as Cl^- homeostasis in neurons (1).

Phosphorylation of specific threonine residues, located within the cytoplasmic N-terminal tail of the cotransporter, leads to its activation (4, 5). These residues are located near the first transmembrane domain and downstream of two R*F*X[V/I] motifs that constitute the binding site for SPAK and OSR1, two mammalian Ste20p-like kinases (6). Binding of the Ste20 kinases is a prerequisite for transporter phosphorylation and activation (7). R*F*X[V/I] motifs are also found in WNK kinases as well as a variety of other proteins (8–10). To bind to their substrates, SPAK and OSR1 utilize a unique protein fold or domain (called CCT (11) or PF2 (12)). This domain is located at their extreme C terminus and is formed by 90 amino acid resi-

* This work was supported by National Institutes of Health Grant DK093501 from the NIDDK (to E. D. and P. A. W.).
[1] Supported by a Foundation for Anesthesia Education and Research grant.
[2] To whom correspondence should be addressed: Dept. of Anesthesiology, Vanderbilt University School of Medicine, T-4202 Medical Center North, 1161 21st Ave. South, Nashville, TN 37232. Tel.: 615-343-7409; Fax: 615-343-3916; E-mail: eric.delpire@vanderbilt.edu.

[3] The abbreviations used are: NKCC1, Na-K-2Cl cotransporter 1; ANOVA, analysis of variance; Cab39, calcium-binding protein 39; DRG, dorsal root ganglion; OSR1, oxidative stress-responsive kinase 1; SPAK, Ste20-related proline/alanine-rich kinase; WNK4, with no K (lysine) member 4.

dues (6). The crystal structure of this domain revealed the presence of a hydrophobic pocket that accommodates the RF*X*[V/I] peptide (11).

The mechanism by which WNK and Ste20 kinases affect NKCC1 function was resolved using *Xenopus laevis* oocytes, one of the most reliable heterologous expression systems. The advantage of the oocyte system is the low expression level of transporters and signaling molecules, which consequently requires reconstitution of signaling cascades one player at a time. Thus, injection of SPAK cRNA alone or WNK4 cRNA alone in oocytes expressing NKCC1 had no effect on NKCC1 function whereas co-expression of both kinases resulted in a severalfold activation of NKCC1 activity (13). As expression of constitutively active SPAK/OSR1 results in cotransporter activation in the absence of WNK4, the current model is that WNK kinases acts upstream of SPAK/OSR1 which act on NKCC1. This model, which has been expanded to NKCC2 and NCC, is supported by both biochemical data (5, 14) and animal models (15–18).

Recently, a scaffolding protein distantly related to armadillo proteins named Cab39 (Calcium-binding protein 39 or MO25 for mouse protein 25), has been demonstrated to enhance the WNK4/SPAK-mediated phosphorylation of NCC and NKCC1 (19, 20). Cab39 was proposed to facilitate the structural changes in SPAK/OSR1 that lead to a closed or active conformation of the kinases upon phosphorylation of T-loop residue by WNK4. Using a concatamer approach, we discovered that Cab39 facilitates activation (T-loop phosphorylation) of SPAK/OSR1 dimers, bypassing the requirement for upstream WNK4 activation (21). Kinase dimerization is consistent with the resolution of the crystal structure of the catalytic domain of OSR1, which showed evidence for domain swapped dimers (12, 22). It has not been tested whether Cab39 similarly activates WNK4 in the absence of SPAK.

In this study, we show that WNK4 possesses a structure that resembles the CCT/PF2 domain of SPAK and OSR1, allowing the kinase to bind directly to the N terminus of NKCC1. In the presence of Cab39, the interaction allows WNK4 to activate NKCC1 in a SPAK-independent manner. WNK4/Cab39 had identical stimulatory effects on NKCC2, indicating that this novel mode of regulation might also be relevant to Na^+ reabsorption mechanisms in the kidney tubule. These data expand the signaling mechanisms that control sodium chloride cotransporter activation and provide a molecular insight to explain how salt transport can be regulated by divergent physiological stimuli.

EXPERIMENTAL PROCEDURES

Molecular Reagents—Full-length cDNAs encoding mouse NKCC1, rat NKCC2, mouse SPAK, mouse WNK4, and mouse Cab39 in the oocyte-expressing vector, pBF, or in the yeast two-hybrid analysis vectors, pGBDUc2 and pACT2, have been described in earlier studies (6, 8, 13, 21, 23). Single amino acid mutations were inserted in clones using the QuikChange Mutagenesis kit from Stratagene, according to the manufacturer's instructions. All clones were sequenced to ensure the presence of desired mutations.

cRNA in Vitro Transcription—Complementary DNA (20 μg) encoding for mouse NKCC1, NKCC2, WNK4, Cab39, SPAK and *X. laevis* Cab39-like and subcloned into the *X. laevis* oocyte expression vector pBF were linearized by incubation at 37 °C overnight with 30 units of the restriction endonuclease MluI (New England Biolabs), purified using a QIAquick PCR Purification kit (Qiagen), and transcribed into cRNA using a mMESSAGE mMACHINE SP6 transcription kit (Invitrogen). cRNA was then purified by using the RNeasy Mini kit (Qiagen) and eluted in diethylpyrocarbonate-treated water. RNA preparation was assessed for quality and quantity through denaturing agarose gel electrophoresis and spectrometric methods.

Isolation and Microinjection of X. laevis Oocytes—All experiments involving animals were approved by the Vanderbilt Institutional Animal Care and Use Committee. Female *X. laevis* frogs were anesthetized by immersion in 1.7 g/liter Tricaine buffered with 3.4 g/liter $NaHCO_3$. Ovarian lobes were surgically externalized and removed, and individual oocytes were dissociated using collagenase D treatment (5 mg/ml; Sigma). Oocytes were maintained overnight in modified L15 solution (250 ml of Leibovitz L15 Ringer (Invitrogen), 200 ml of deionized water, 952 mg of HEPES (acid form), and 44 mg/liter gentamycin (Invitrogen), pH 7.4, 195–200 mosM) at 16 °C. The following day, groups of 25 oocytes were injected with 50 nl containing 15 ng of Na-K-2Cl cotransporter 1 (NKCC1) or NKCC2 and returned to the incubator. On day 3, they were injected with 50 nl of water containing cRNA encoding regulatory proteins (10 ng each). Western blot analysis and ^{86}Rb tracer flux studies to measure Na-K-2Cl cotransport expression and function, respectively, were assessed on day 5.

K^+ Influx Measurements—Groups of 20–25 oocytes were placed in 35-mm dishes, washed once with 3 ml of isosmotic saline (96 mM NaCl, 4 mM KCl, 2 mM $CaCl_2$, 1 mM $MgCl_2$, 5 mM HEPES buffered to pH 7.4, 200 mosM), and preincubated for 15 min in 1 ml of the same solution containing 1 mM ouabain. The solution was then aspirated and replaced with 1 ml of isosmotic flux solution containing 5 μCi of ^{86}Rb. Two aliquots (5 μl each) of flux solution were sampled at the beginning of each uptake period and used as standards. After a 1-h uptake, the radioactive solution was aspirated, and the oocytes were washed four times with 3 ml of ice-cold isosmotic solution. Single oocytes were transferred into glass vials, lysed for 1 h with 200 μl of 0.25 N NaOH, and neutralized with 100 μl of glacial acetic acid, and tracer activity was measured by β-scintillation counting. Previous work has shown that >90% of K^+ influx is mediated by NKCC1.

Immunoprecipitation—Stage V–VI *X. laevis* oocytes were isolated on day 1 and kept at 16 °C for 5 days. Oocytes were microinjected with 15 ng of c-myc-NKCC1 on day 2 and 15 ng of HA-WNK4 on day 3 (c-myc-tag: N-Glu-Gln-Lys-Leu-Ile-Ser-Glu-Glu-Asp-Leu-C; HA-tag: N-Tyr-Pro-Tyr-Asp-Val-Pro-Asp-Tyr-Ala-C). A group of oocytes was injected with HA-WNK4 only to serve as negative control. On day 5, oocytes were homogenized by passing them through a pipette tip in 20 μl/oocyte radioimmunepreciptation assay buffer (150 mM NaCl, 50 mM Tris-Cl, 0.5 mM EDTA, 1% Nonidet P-40, 1% sodium deoxycholate, 0.1% sodium dodecyl sulfate), supplemented with Complete™ Protease Inhibitor Mixture Tablet,

EDTA-free (Roche Applied Science). Homogenates were incubated on ice for 20 min, centrifuged at 15,000 × *g* for 15 min at 4 °C, and supernatants were recovered. Immunoprecipitation was achieved by adding 7 μl of anti-c-myc antibody to 200 μl of lysate (*i.e.* ~10 oocytes) brought to 1 ml with radioimmunoprecipitation assay buffer, under gentle rotation overnight at 4 °C. The following day, 30 μl of pre-washed protein A-Sepharose (Santa Cruz Biotechnology) was added to each homogenate and incubated for 2 h at 4 °C. The Sepharose beads (immunoprecipitate) were washed three times with 1 ml of lysis buffer, and the immunoprecipitates were resuspended in 100 μl of 2× sample buffer containing 60 mM dithiothreitol, heated at 75 °C for 15 min. Following centrifugation, 90 μl of sample was subjected to SDS-PAGE.

Western Blot Analyses—For the phospho-NKCC1 experiment, a large group of oocytes was injected with 15 ng of NKCC1 cRNA and randomized into five experimental groups. The following day, two groups were injected with water, one group with 10 ng of WNK4 cRNA, one group with 10 ng of Cab39 cRNA, and one group with 10 ng of WNK4 cRNA and Cab39 cRNA, each. After 2 additional days, the oocytes were treated or not with a hyperosmotic (265 mosM) solution for 15 min, then lysed with 20 μl/oocyte lysis buffer (150 mM NaCl, 30 mM NaF, 5 mM EDTA, 15 mM pyrophosphate, 15 mM Na_2HPO_4, 1 mM Na_3VO_4, 20 mM HEPES, pH 7.2, 1% Triton X-100) supplemented with protease inhibitors (Roche Applied Science). To test for expression of the wild-type and mutant WNK4 kinases, cRNA encoding HA-tagged WNK4 kinases were injected in oocytes, and 2 days later, the oocytes were lysed with 20 μl/oocyte lysis buffer (100 mM NaCl, 50 mM Tris-Cl, pH 7.6, 5 mM EDTA, 1% Triton X-100, 0.1% SDS) supplemented with protease inhibitor tablet (Roche Applied Science). Equal amount of lysate was then separated on a gradient gel (polyacrylamide from 3 to 12%).

All gels were transferred to polyvinylidine fluoride membranes (PVDF; Millipore). The membranes were blocked in Tris-buffered saline, 0.5% Tween 20 (TBST) with 5% milk for 2 h at room temperature and subjected to affinity-purified sheep anti-phospho-NKCC1 (S763B; phospho-T203 + T207 + T212 antibody from MRC, Dundee, Scotland) in the presence of unphosphorylated peptide or HRP-conjugated rat anti-HA antibody (Clone 3f10; Roche Applied Science), overnight at 4 °C. For NKCC1, after extensive washes in TBST, the membrane was incubated with an HRP-conjugated anti-sheep secondary antibody (Jackson ImmunoResearch Laboratories) for 1 h at room temperature, washed again extensively in TBST, and protein bands were visualized using enhanced chemiluminescence (ECL Plus; Amersham Biosciences).

Computational Modeling—In a first step, the primary sequence of the PF2-like domain of WNK4 was aligned with the PF2 domain of OSR1 using ClustalW and then threaded over a template based on the crystal structure of the PF2 domain of OSR1 (2v3s) utilizing a python script supplied in the Rosetta software suite (version 3.4.1) (24). Fragment files of the PF2-like sequence were then generated through the use of the Rosetta server. After creation of the appropriate files (24), 10,000 comparative models of the PF2-like domain were generated using the Rosetta loop modeling modality (25). The top 500 scoring models were then clustered based on root mean square deviation to 2.0 Å (26), and the top 10 comparative models based on Rosetta energy and clustering were selected for peptide docking. In a second step, for each of the models, the Gly-Arg-Phe-Gln-Val-Thr hexapeptide was manually placed into the PF2-like domain that corresponded to the CCT-binding pocket of OSR1 using PyMOL (PyMOL Molecular Graphics System, Version 1.5.0.4, Schrödinger, LLC). The peptide was then docked into the binding pocket through the use of the FlexPepDock application of Rosetta with standard flags as noted by Raveh *et al.* (27), and a Rosetta binding energy ($\Delta\Delta G_{binding} = \Delta G_{TS\_bound} - \Delta G_{unbound}$) was calculated. This process was repeated for PF2-like F473A mutant. Finally, the Gly-Arg-Phe-Gln-Val-Thr hexapeptide was also computationally docked using FlexPepDock as previously stated into the crystal structure of the PF2 domain of OSR1 to determine relative energies.

Yeast Two-hybrid assays—The entire open reading frames of Cab39 and Cab39 mutants were subcloned downstream of the binding domain of GAL4 in the vector pGBDUc2. The clones were transformed into competent PJ69-4A yeast (28) and plated on uracil-deficient agar plates. Surviving yeast cells containing wild-type or mutated Cab39 were then transformed a second time with different protein fragments inserted downstream of the activating domain of GAL4 in pACT2. These fragments consisted of the regulatory domain of SPAK (amino acids 353–546), full-length WNK4, and the cytosolic N-terminal domain of NKCC1 (amino acids 1–278). The yeast transformants were then plated on double dropout (−uracil, −leucine) plates for measuring transformation efficiency and triple dropout (−uracil, −leucine, −histidine) plates for determining protein-protein interaction. Yeast survival was assessed after 1–2 days (fast growth) and 4–5 days (slow growth) at 30 °C. The SPAK and WNK4 fragments were also subcloned in pGBDUc2 for additional yeast two-hybrid experiments.

RESULTS

WNK4-Cab39 Activates NKCC1 and NKCC2 in the Absence of SPAK—To explore the involvement of Cab39 in WNK-dependent regulation of NKCC, co-expression studies were performed in *X. laevis* oocytes. We found that NKCC1-mediated K^+ influx was not affected by the expression of either WNK4 or Cab39 alone (Fig. 1*A*, *first four bars*), consistent with the requirement of multiple components. Surprisingly, however, coexpression of WNK4 and either Cab39 (*fifth bar*) or Cab39-like (*sixth bar*, MGI: 1914081, a protein that is 79% identical to Cab39) resulted in a significant increase (3–5-fold) in K^+ transport in the absence of exogenous SPAK. The WNK4-Cab39-mediated increase in K^+ transport was completely attributable to NKCC1 function, as it is inhibited by addition of 20 μM bumetanide (Fig. 1*A*, *seventh bar*). Similar data were obtained with rat NKCC2 (Fig. 1*B*, *second through sixth bars*). As indicated at the top of *A*, the WNK4 + Cab39 activation of NKCC1 was associated with significant phosphorylation of the cotransporter at residues Thr-203, Thr-207, and Thr-212. Consistent with the flux, no activation was observed with WNK4 or Cab39 alone. Oocytes treated with a hypertonic solution served as positive controls.

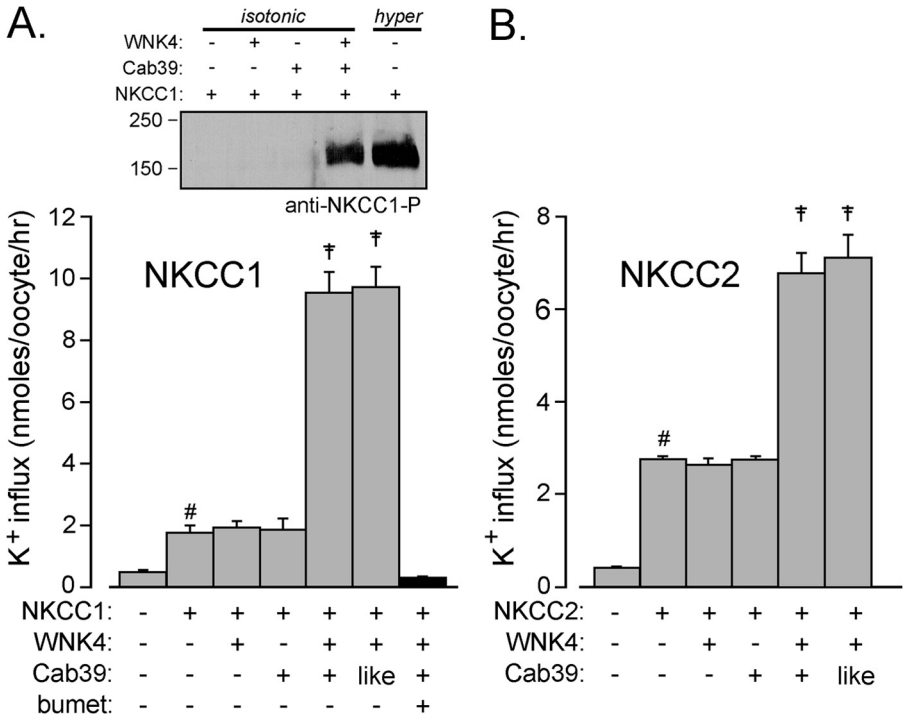

FIGURE 1. **WNK4 activates NKCC-mediated K^+ influx in the presence of Cab39.** *A*, K^+ uptake under isosmotic conditions (200 mosM) in *X. laevis* oocytes injected with NKCC1, WNK4, Cab39, or Cab39-like cRNAs. Bumetanide, 20 μM. *Inset*, Western blot analysis of phospho-NKCC1 with groups of 20 oocytes injected with NKCC1 in the presence of absence of WNK4, Cab39, or WNK4 + Cab39. *B*, K^+ uptake under isosmotic conditions in oocytes injected with NKCC2, WNK4, Cab39, or Cab39-like cRNAs. *Bars* represent mean ± S.E. (*error bars*; $n = 20–25$ oocytes). #, Flux measured in NKCC-injected oocytes is significantly greater than flux in water-injected oocytes ($p < 0.001$, ANOVA). ‡, WNK4 in the presence of Cab39 or Cab39-like activates NKCC ($p < 0.001$, ANOVA). Fluxes are expressed in nmol of K^+ per oocyte per h.

To assess whether the catalytic activity of WNK4 was required, we coexpressed a catalytically inactive mutant of WNK4 (WNK4-K183M; see model in Fig. 2*B*) with Cab39. No activation was observed with the kinase-deficient mutant (Fig. 2*A*, *second bar*). To test whether the endogenous OSR1 mediates the WNK4-Cab39-mediated activation of NKCC1, we coexpressed WNK4 and Cab39 with SPAK-K104R, a catalytically inactive form of SPAK, which acts as a dominant negative to SPAK and OSR1 (13). As shown in Fig. 2*A*, *third and fourth bars*, catalytically inactive SPAK decreased the level of K^+ uptake in NKCC1-injected oocytes, but did not prevent cotransporter activation by WNK4 + Cab39. Furthermore, because we previously demonstrated that binding between WNK4 and SPAK was required for WNK4 activation of SPAK and that the binding could be prevented by mutation of residue Phe-997 into alanine (13), we tested the Phe-997 mutant with Cab39 on NKCC1 function. We found that mutation of residue Phe-997 did not affect the WNK4 ability to activate NKCC1 in the presence of Cab39 (*fifth bar*), confirming that the stimulation is independent of SPAK. For completeness, we verified that the WNK4-binding mutant WNK4 was unable to activate the cotransporter through SPAK (*sixth bar*). Western blot analysis confirmed expression of wild-type and K183M mutant WNK4 proteins (*inset*, Fig. 2*A*).

WNK4 Interacts with NKCC1 RFX[V/I] Motif—We previously reported sequence (29) and structural (30) similarities between a portion of the CCT/PF2 domain of SPAK/OSR1, which is involved in binding RF*X*[V/I] peptides, and a region of WNK4 located immediately downstream of the catalytic domain (residues 467–504). Consequently, we considered the possibility that this PF2-like domain promotes direct WNK4 interaction with RF*X*[V/I] motifs in NKCC1. First, through the use of the Rosetta modeling suite (31), the PF2-like domain of WNK4 was folded utilizing the crystal structure of the CCT domain of OSR1 as its template. The original Gly-Arg-Phe-Gln-Val-Thr hexapeptide located in the binding pocket of the crystal structure of the CCT domain was then docked into the corresponding pocket formed in the WNK4 PF2-like domain (Fig. 3, *A* and *B*). This peptide was similarly redocked into the native CCT/PF2 domain of OSR1 to provide reference energies (Fig. 3*C*). As shown in Table 1, the hexapeptide interacted with the PF2-like domain with slightly less affinity (more positive $\Delta\Delta G$) compared with the native CCT domain. However, the individual binding energies of the RF*X*V portion of the two motifs were extremely similar, varying from one another by less than 0.03 Rosetta energy units. Altering the Phe to an Ala in the PF2-like domain (F473A) significantly destabilizes the bound complex and particularly affects the binding of the hexapeptide phenylalanine (Table 1). In addition, the wild-type phenylalanine at position 473 of the receptor maintains an individual ddG of −0.945 compared with −0.304 of the mutant alanine at the same position, further signifying a destabilized variant.

To test the interaction experimentally, we used the yeast two-hybrid method and indeed observed a direct interaction between WNK4 and NKCC1 (Fig. 4*A*, condition 1). To assess whether the PF2-like domain participates in binding, we mutated a phenylalanine residue in WNK4 (F473A) critical in forming the hydrophobic pocket which accommodates the

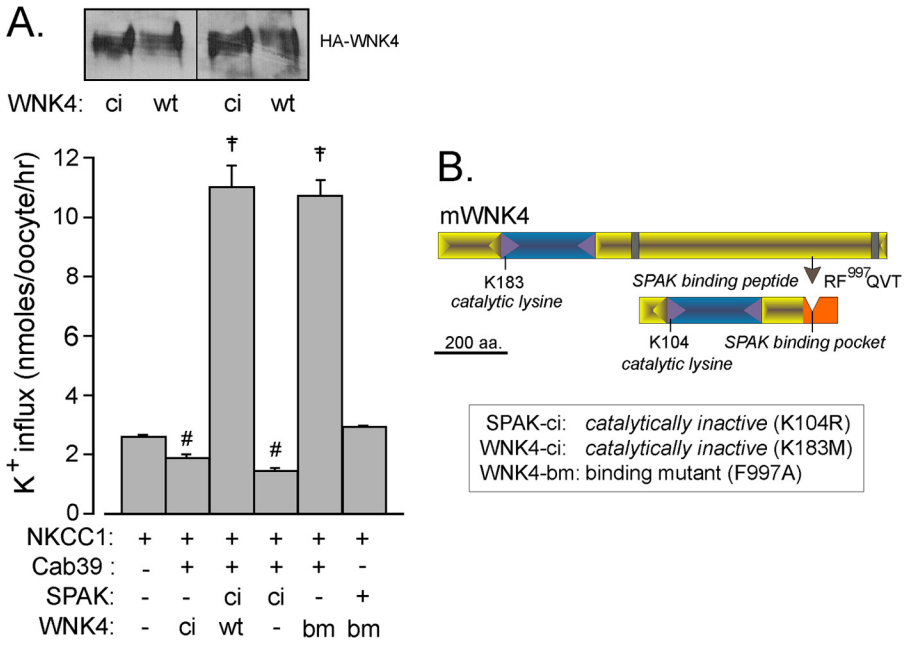

FIGURE 2. **WNK4 activation requires catalytic activity and is SPAK-independent.** *A*, K^+ uptake was measured under isosmotic conditions in oocytes injected with NKCC1, Cab39, catalytically inactive (*ci*; K183M) WNK4, catalytically inactive (*ci*; K104R), SPAK, and SPAK-binding deficient (F997A) WNK4 mutant cRNAs. *Bars* represent mean ± S.E. (*error bars*; $n = 20–25$ oocytes). #, Flux in oocytes injected with dominant negative kinases is significantly less than flux under control conditions ($p < 0.001$, ANOVA). ‡, WNK4 in the presence of Cab39 activates NKCC in the presence of overexpression of catalytically inactive SPAK ($p < 0.001$, ANOVA). Fluxes are expressed in nmol of K^+ per oocyte per h. *Inset*, Western blot analysis confirms that wild-type and catalytically inactive (K183M) WNK4 kinases (*second and third bars* in *A*) are expressed in the oocytes. *B*, schematic represents kinases with catalytic (*blue*) and regulatory domains (*yellow*) and key residues targeted for mutagenesis.

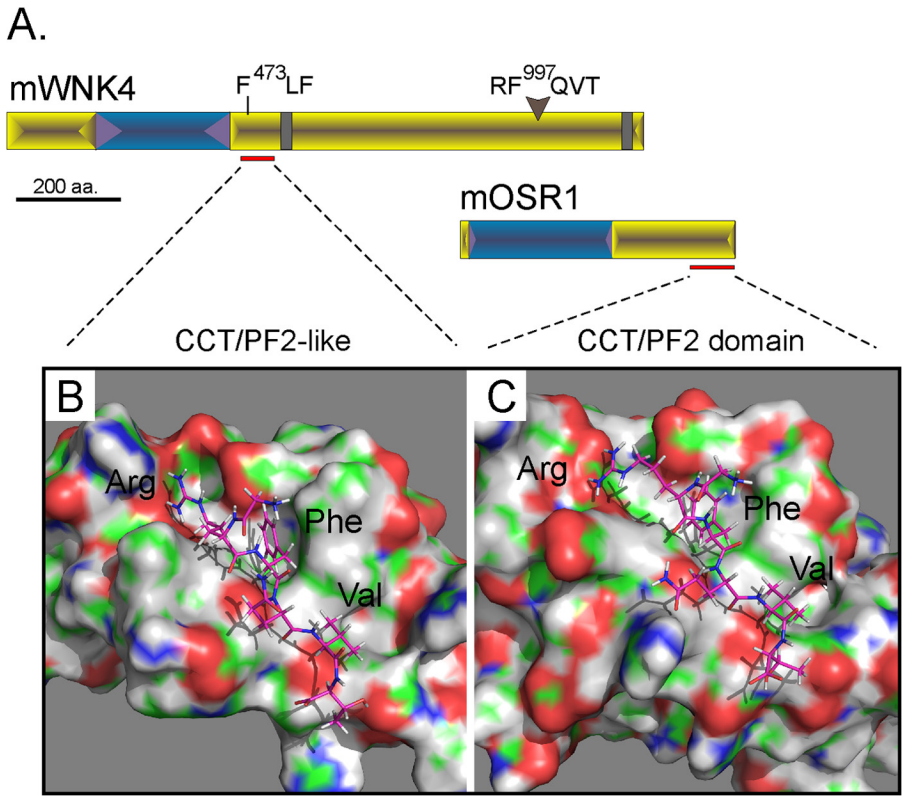

FIGURE 3. **Conservation of RF*X*V-binding pocket between OSR1-PF2 and WNK4-PF2-like domains.** *A*, schematic representation of WNK4 and OSR1 kinases with catalytic (*blue*) and regulatory domains (*yellow*) and location of the PF2 domains (red line). The SPAK binding domain on WNK4 (RFQVT peptide) also indicated. *B*, Rosetta modeling of the CCT/PF2-like domain of WNK4 with GRFQVT peptide located in hydrophobic pocket. *C*, for comparison, the OSR1 CCT/PF2 domain with GRFQVT peptide from the crystal structure. The surface representation of the domains highlights negative (*red*), positive (*blue*), and polar (*green*) moieties.

TABLE 1
Binding energies (ΔΔ*G*) of CCT and CCT-like domains
The free energy of binding (ΔΔ*G*) value, given in Rosetta energy units, provides a measure of binding affinity of a substrate to its receptor.

	Hexamer (or total)	Glycine (−1)	Arginine (+1)	Phenylalanine (+2)	Glutamine (+3)	Valine (+4)	Threonine (+5)
PF2 (OSR1)	**−17.59**	0.002	−1.504	−2.356	−2.553	−0.831	−0.523
PF2-like (WNK4)	**−16.62**	−0.010	−1.765	−2.323	−2.288	−0.895	−0.461
PF2-like (WNK4) F473A	**−14.48**	−0.015	−2.059	−1.084	−2.132	−0.853	−0.447

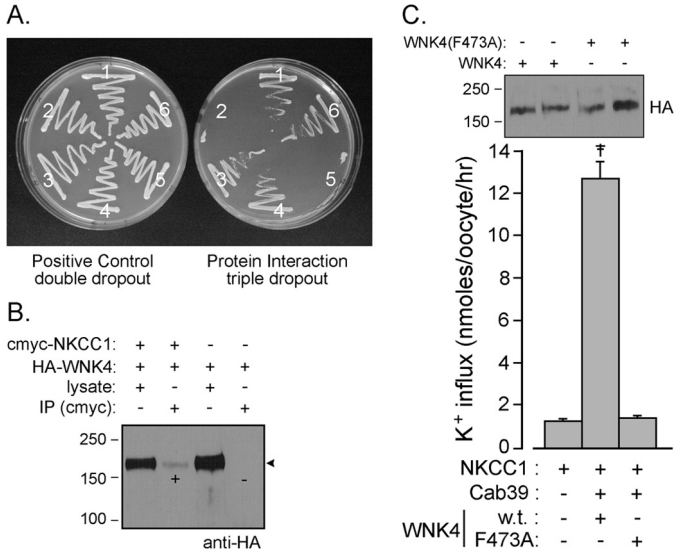

FIGURE 4. **Effect of WNK4 on NKCC1 is binding-dependent.** *A*, yeast two-hybrid analysis showing yeast growth at 30 °C in triple dropout plates when transfected with NKCC1-NT and WNK4 (condition 1), Cab39 and WNK4 (condition 3), Cab39 and SPAK (condition 4), and NKCC1 and SPAK (condition 6). No growth is detected with yeast transfected with NKCC1 and WNK4-F473A mutant (condition 2), and Cab39 and NKCC1-NT (condition 5). As positive control, all yeasts survived in double dropout plates, indicating that both bait and prey vectors are properly transfected in the yeast. *B*, coimmunoprecipitation of WNK4 with NKCC1. Oocytes were injected with NKCC1 and WNK4 or WNK4 alone. Western blot demonstrates that WNK4 was expressed in both conditions (*first and third lanes*). When NKCC1 was immunoprecipitated, WNK4 was observed (*second lane*). As a negative control, there was no WNK4 signal in the absence of NKCC1 (*fourth lane*). Both NKCC1 and WNK4 were epitope-tagged, as indicated in the *panel*. *C*, K^+ uptake measured under isosmotic conditions in oocytes injected with NKCC1, Cab39, wild-type WNK4, and binding-deficient (F473A) mutant WNK4 cRNAs. *Bars* represent mean ± S.E. (*error bars*; $n = 20–25$ oocytes). ‡, WNK4 in the presence of Cab39 activates NKCC1 ($p < 0.001$, ANOVA). Fluxes are expressed in nmol of K^+ per oocyte per h. *Inset* demonstrates that wild-type and mutant WNK4 proteins were expressed in the oocytes.

RF*x*[V/I] peptide (Table 1). Interaction was prevented by this F473A mutation (condition 2). We also tested interaction between Cab39 and WNK4 (condition 3), Cab39 and SPAK (condition 4), Cab39 and NKCC1 (condition 5), as well as SPAK and NKCC1 (condition 6, as positive control). We show that the adaptor protein tightly binds to the two kinases, but does not interact with the N-terminal regulatory tail of the cotransporter. Direct interaction of WNK4 with NKCC1 was also demonstrated by coimmunoprecipitation (Fig. 4*B*). Epitope-tagged WNK4 (HA-WNK4) was immunoprecipitated with NKCC1 from oocytes expressing the c-myc-tagged NKCC1 (*second lane*), but not from oocytes expressing WNK4 alone (*fourth lane*). Input samples (*first and third lanes*) demonstrate that the kinase was expressed in both groups of oocytes. Finally, consistent with disruption of binding, the WNK4-F473A mutant was unable to activate NKCC1 in the presence of Cab39 (Fig. 4*C*).

Cab39 Interacts Differentially with SPAK, LKB1, and WNK4—Previous studies have demonstrated that Cab39 residues Met-260 and Lys-297 play important roles in sustaining interaction with STRADα, a pseudo-kinase belonging to the Ste20 family (32). To assess the role of these residues toward SPAK and WNK4 binding, we performed additional yeast two-hybrid analyses and demonstrated that alanine substitutions of either or both amino acids inhibited the interaction with SPAK (Fig. 5*A*, *top*). In contrast, the interaction between WNK4 and Cab39 was unaffected by the single or double mutations (Fig. 5*A*, *bottom*). Accordingly, the mutations did not prevent activation of NKCC1 by WNK4-Cab39 (Fig. 5*B*). These data indicate that Cab39 binds to STRADα and SPAK similarly, but to WNK4 differently.

Studies have also demonstrated that residue Arg-240 in Cab39 facilitate the interaction of the adaptor protein with LKB1/STK11, a master serine/threonine kinase involved in energy metabolism, cell polarity, and cell growth (33). As mutation of this residue into alanine did not prevent cotransport activation by WNK4-Cab39, we conclude that Cab39 also interacts with WNK4 differently than with LKB1.

A Single Amino Acid WNK4 Mutant Distinguishes the WNK4/SPAK Pathway from the WNK4/Cab39 Pathway—Because a recent report showed that an acidic domain located upstream of the PF2-like-binding pocket was responsible for calcium sensitivity of WNK4 (34), we tested whether mutation of this acidic domain affected the WNK4-Cab39 activation of NKCC1. We found that mutating glutamic acid residue 559 into a lysine abrogated the WNK4-Cab39 activation of NKCC1 (Fig. 6, *sixth bar*). In contrast, we found that the E559K mutant conserved its catalytic activity and its ability to activate SPAK. Indeed, coexpression of WNK4-E559K with SPAK (*fourth bar*) activated NKCC1 activity to the same extent as coexpression of wild-type WNK with SPAK (*third bar*). These data indicate that the acidic domain is involved in the WNK4-Cab39 activation of NKCC1, but not in the WNK4-SPAK activation of the cotransporter.

DISCUSSION

The last ~90 C-terminal residues of SPAK and OSR1 form an interaction structure called the CCT/PF2 domain (6, 11). Although the domain has been thought to be unique to SPAK and OSR1, we noticed sequence homology between 58 residues of this CCT/PF2 domain and a region of WNK4, which is located downstream of the catalytic domain (29). Rosetta modeling revealed structural homology between the domain in WNK4 and the hydrophobic pocket of the CCT/PF2 domain. Remarkably, the three-dimensional conformation of the two binding pockets are separated by root mean square deviation of only 0.603 Å, indicating that the RF*X*V peptide is highly likely to

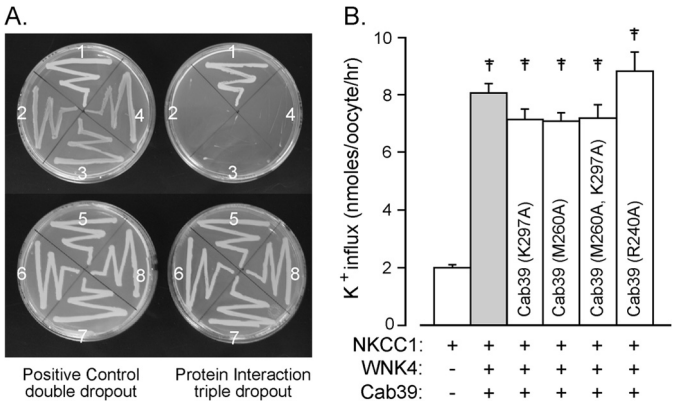

FIGURE 5. **Cab39 interacts differentially with SPAK and WNK4.** *A*, yeast two-hybrid analysis showing interaction of SPAK with wild-type Cab39 (condition 1), but not with SPAK and mutant K297A (condition 2), M260A (condition 3), and K297A + M260A (condition 4) mutant Cab39 proteins. In contrast, WNK4 interacts with wild-type and mutant Cab39 (conditions 5–8). As positive control, all yeasts survive in double dropout plates. *B*, K^+ uptake measured under isosmotic conditions in oocytes injected with NKCC1, WNK4, and Cab39 mutant cRNAs. *Bars* represent mean ± S.E. (*error bars*; $n = 20–25$ oocytes). ‡, WNK4 in the presence of all Cab39 proteins activates NKCC1 ($p < 0.001$, ANOVA). Fluxes are expressed in nmol of K^+ per oocyte per h.

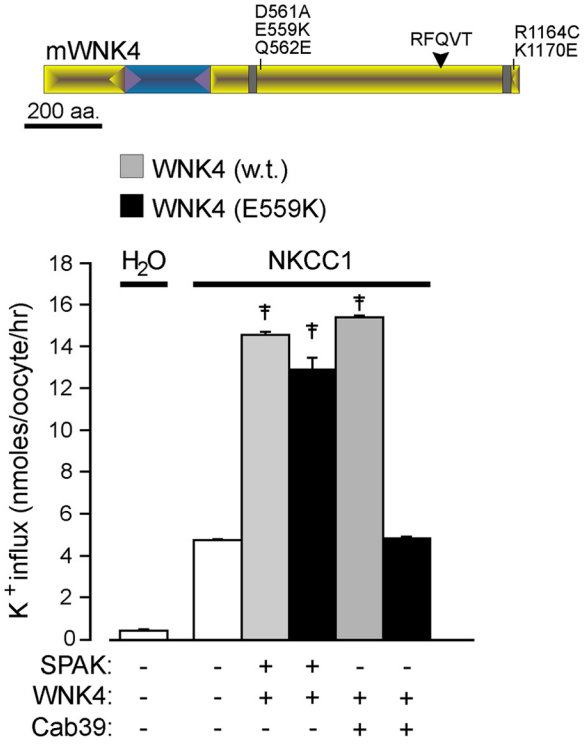

FIGURE 6. **Differential effect of the acidic domain WNK4-E559K mutant when coexpressed with Cab39 or SPAK.** K^+ uptake was measured under isosmotic conditions in oocytes injected with NKCC1 in the absence or presence of various regulatory proteins. Note that E55K mutant WNK4 (*black bars*) is able to promote activation of NKCC1 in the presence of SPAK but not in the presence of Cab39, whereas wild-type WNK4 (*gray bars*) is able to activate the cotransporters in the presence of SPAK or Cab39. *Bars* represent mean ± S.E. (*error bars*; $n = 20–25$ oocytes). ‡, WNK4 in the presence of all Cab39 proteins activates NKCC1 ($p < 0.001$, ANOVA). Fluxes are expressed in nmol of K^+ per oocyte per h. *Top*, model of WNK4 showing the catalytic domain (*blue*) and regulatory domains (*yellow*) with PHAII mutations highlighted. The position of the SPAK (RFQVT)-binding domain is also indicated.

bind to this region of WNK4. This observation prompted us to examine the possibility that WNK4 directly interacts and activates NKCC1. Our experiments were also guided by the knowledge that Cab39, an adaptor protein, facilitates kinase activity (19, 20). We thus examined the role of WNK4 in the presence of Cab39. Our current data show that neither WNK4 nor Cab39 affected NKCC1 or NKCC2 activity, but when combined, WNK4 and Cab39 are able to mediate activation of both cotransporters. We do not believe that the activation occurs through the native oocyte OSR1 kinase for the following reasons. First, if OSR1 is sufficiently expressed in oocytes, why does expression of WNK4 through cRNA injection not lead to cotransporter activation? If it is that Cab39 is also required for this activation, why then cotransporter activation by exogenous SPAK/OSR1 and WNK4 does not require Cab39? Second, we coinjected catalytically inactive SPAK to act as a dominant negative kinase and whereas a dominant negative effect was observed in the absence of WNK4, full stimulation was still observed when catalytically inactive SPAK was coinjected with WNK4 and Cab39. Third, we know that the WNK4-mediated SPAK/OSR1 activation requires interaction between the two kinases, and we know that this interaction occurs at an RF*X*V SPAK/OSR1-binding site located in the regulatory domain of WNK4. We show here that when SPAK is coinjected with a WNK4 mutant that is deficient in SPAK binding, no activation is observed. Thus, we would expect this WNK4 mutant not to interact with native OSR1. However, this mutant WNK4 is still able to activate NKCC1 in the presence of Cab39. Fourth, we show using yeast two-hybrid analysis that WNK4 interacts directly with the N-terminal tail of NKCC1 and that this interaction is prevented by mutating a key phenylalanine residue (Phe-473) located in the conserved hydrophobic pocket that binds RF*X*V peptides. Consequently, this mutant WNK4 kinase is unable to mediate activation of the cotransporter in the presence of Cab39. We also confirmed direct interaction between the kinase and the cotransporter by coimmunoprecipitation. A direct interaction between WNK4 and NCC, a related cation-chloride cotransporter, has also been previously demonstrated (35). Fifth, we show differential effects of E559K mutation on the SPAK-dependent WNK4 activation *versus* the SPAK-independent WNK4/Cab39 activation of NKCC1. Indeed, we observed that the WNK4-E559K kinase is catalytically activate and able to mediate NKCC1 activation when SPAK is coinjected in the oocytes, whereas it is unable to activate the cotransporter in the presence of Cab39 when SPAK is not coinjected. Thus, our data clearly indicate that the WNK4-Cab39 stimulation of NKCC1 constitutes a different activation pathway than the WNK4-SPAK pathway (Fig. 7).

To make the matter even more complex, we also demonstrated in a 2012 paper that SPAK functions as a dimer, and when coexpressing Cab39 with a SPAK concatamer in *X. laevis* oocytes, we were able to obtain activation of NKCC1 in the absence of WNK4 (21). This pathway is also depicted in Fig. 7. Thus, in heterologous expression system, we were able to demonstrate three pathways: a WNK4-dependent SPAK pathway, a WNK4-independent SPAK pathway, and now a SPAK-independent WNK4 pathway. To this we can add the inhibitory effect of WNK4 on cotransporter expression observed in some studies (35). It seems therefore that there are many ways that kinases can be activated and many pathways to cotransporter

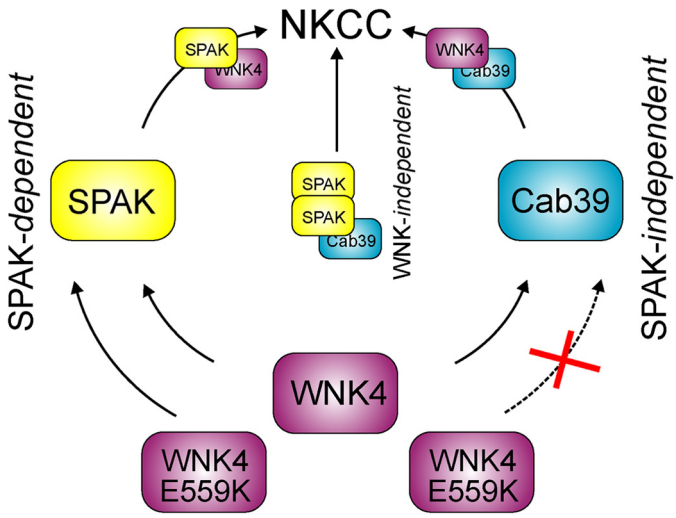

FIGURE 7. **Model showing three pathways of NKCC activation.** On the *left side*, we illustrate the traditional pathway where WNK4 interacts and phosphorylates SPAK leading to activation of NKCC. Mutation of WNK4 (E559K) does not affect this pathway. In the *middle*, we show a pathway where Cab39 facilitates intermolecular SPAK activation in the absence of WNK4. On the *right side*, we depict the novel pathway involving WNK4 and Cab39. In this case, mutation of WNK4 at glutamic acid 559 prevents activation of this pathway.

activation. The challenge will be to identify under which physiological condition which particular pathway is involved *in vivo*.

Cab39 and Cab39-like are widely expressed adaptor proteins. Thus, their expression likely overlaps with WNK4 expression. We have, for instance, demonstrated that WNK4 is expressed in a rat dorsal root ganglion (DRG) cell line (50B11 cells) as well as in native mouse sensory DRG neurons (36). Using a Cab39 antibody and Western blot analysis, we observed expression of the adaptor protein in 50B11 cells and native mouse sensory DRG neurons (data not shown). Furthermore, we showed in a 2012 study that Cab39 is present in nephron segments where WNK4 is expressed (18). Thus, the ubiquitous expression of the two Cab39 adaptor proteins speaks for the critical role they play in facilitating the activation of many kinases.

Our study has uncovered a critical role for Cab39 in WNK4 function. Our yeast two-hybrid data clearly show that the adaptor protein interacts with the WNK4 kinase. It is tempting to speculate that the "unidentified" 40-kDa protein that was reported in a previous study to bind to WNK4 (37) is in fact Cab39. This 40-kDa protein was assumed to be a kinase because it induced OSR1 phosphorylation when bound to a catalytically deficient WNK4. However, because Cab39 binding to kinases greatly affects their catalytic function, it is conceivable that Cab39 significantly increased the catalytic activity of the WNK4 mutant. The site of interaction between Cab39 and WNK4 is still unknown, but likely to occur in the C-terminal regulatory domain. When we mutated two Cab39 residues that were shown to interact with the Ste20 pseudo-kinase STRADα, interaction with SPAK but not WNK4 was lost, indicating that the WNK kinase interacts differently with Cab39 than Ste20 kinases. To assess whether WNK4 forms a complex with Cab39 similar to the one described for LKB1 (STK11), we mutated a critical residue involved in LKB1 binding, and again the Cab39-WNK4 interaction was not affected. These data clearly indicate a different binding modality between the adaptor protein and the WNK kinase. Based on sequence similarity to Ca^{2+} and calmodulin-binding motifs of plasma membrane Ca^{2+}-ATPase, Cab39 has been proposed to bind calcium (38), raising the possibility that Cab39-WNK4 confers a SPAK/OSR1-independent regulatory pathway that couples intracellular calcium to NKCC activation. Such a pathway may explain how purinergic stimulation induces Ca^{2+}-dependent activation of Na^+-K^+-$2Cl^-$ cotransporter (see Ref. 39).

In this study, we not only showed stimulation of NKCC1, but also activation of NKCC2 by WNK4-Cab39, indicating relevance of the SPAK-independent WNK4 activation for renal cotransporters. Although this novel pathway still needs to be tested with NCC, conservation of the RF*X*[V/I]-binding sites and of phosphorylation sites within the N-terminal tails of NKCC1, NKCC2, and NCC strongly suggests relevance of this mode of activation for both the thick ascending limb and the distal convoluted tubule. With respect to NCC, it is worth noting that mutation E559K is found in pseudohypoaldosteronism of type II (PHAII) or Gordon syndrome (40), a human condition that involves increased levels of WNK4 and increased salt reabsorption in the distal convoluted tubule through NCC (41–43).

REFERENCES

1. Gagnon, K. B., and Delpire, E. (2013) Physiology of SLC12 transporters: lessons from inherited human genetic mutations and genetically-engineered mouse knockouts. *Am. J. Physiol. Cell Physiol.* **304,** C693–C714
2. Delpire, E., Lu, J., England, R., Dull, C., and Thorne, T. (1999) Deafness and imbalance associated with inactivation of the secretory Na-K-2Cl co-transporter. *Nat. Genet.* **22,** 192–195
3. Flagella, M., Clarke, L. L., Miller, M. L., Erway, L. C., Giannella, R. A., Andringa, A., Gawenis, L. R., Kramer, J., Duffy, J. J., Doetschman, T., Lorenz, J. N., Yamoah, E. N., Cardell, E. L., and Shull, G. E. (1999) Mice lacking the basolateral Na-K-2Cl cotransporter have impaired epithelial chloride secretion and are profoundly deaf. *J. Biol. Chem.* **274,** 26946–26955
4. Darman, R. B., and Forbush, B. (2002) A regulatory locus of phosphorylation in the N terminus of the Na-K-Cl cotransporter, NKCC1. *J. Biol. Chem.* **277,** 37542–37550
5. Vitari, A. C., Thastrup, J., Rafiqi, F. H., Deak, M., Morrice, N. A., Karlsson, H. K., and Alessi, D. R. (2006) Functional interactions of the SPAK/OSR1 kinases with their upstream activator WNK1 and downstream substrate NKCC1. *Biochem. J.* **397,** 223–231
6. Piechotta, K., Lu, J., and Delpire, E. (2002) Cation-chloride cotransporters interact with the stress-related kinases SPAK and OSR1. *J. Biol. Chem.* **277,** 50812–50819
7. Gagnon, K. B., England, R., and Delpire, E. (2007) A single binding motif is required for SPAK activation of the Na-K-2Cl cotransporter. *Cell Physiol. Biochem.* **20,** 131–142
8. Piechotta, K., Garbarini, N., England, R., and Delpire, E. (2003) Characterization of the interaction of the stress kinase SPAK with the Na^+-K^+-$2Cl^-$ cotransporter in the nervous system: evidence for a scaffolding role of the kinase. *J. Biol. Chem.* **278,** 52848–52856
9. Gagnon, K. B., England, R., Diehl, L., and Delpire, E. (2007) Apoptosis associated tyrosine kinase scaffolding of protein phosphatase 1 and SPAK reveals a novel pathway for Na-K-2C1 cotransporter regulation. *Am. J. Physiol. Cell Physiol.* **292,** C1809–C1815
10. Delpire, E., and Gagnon, K. B. (2007) Genome-wide analysis of SPAK/OSR1 binding motifs. *Physiol. Genomics* **28,** 223–231
11. Villa, F., Goebel, J., Rafiqi, F. H., Deak, M., Thastrup, J., Alessi, D. R., and van Aalten, D. M. (2007) Structural insights into the recognition of substrates and activators by the OSR1 kinase. *EMBO Rep.* **8,** 839–845
12. Lee, S. J., Cobb, M. H., and Goldsmith, E. J. (2009) Crystal structure of domain-swapped STE20 OSR1 kinase domain. *Protein Sci.* **18,** 304–313

13. Gagnon, K. B., England, R., and Delpire, E. (2006) Volume sensitivity of cation-chloride cotransporters is modulated by the interaction of two kinases: SPAK and WNK4. *Am. J. Physiol. Cell Physiol.* **290,** C134–C142
14. Vitari, A. C., Deak, M., Morrice, N. A., and Alessi, D. R. (2005) The WNK1 and WNK4 protein kinases that are mutated in Gordon's hypertension syndrome, phosphorylate and active SPAK and OSR1 protein kinases. *Biochem. J.* **391,** 17–24
15. Rafiqi, F. H., Zuber, A. M., Glover, M., Richardson, C., Fleming, S., Jovanović, S., Jovanović, A., O'Shaughnessy, K. M., and Alessi, D. R. (2010) Role of the WNK-activated SPAK kinase in regulating blood pressure. *EMBO Mol. Med.* **2,** 63–75
16. Yang, S. S., Lo, Y. F., Wu, C. C., Lin, S. W., Yeh, C. J., Chu, P., Sytwu, H. K., Uchida, S., Sasaki, S., and Lin, S. H. (2010) SPAK-knockout mice manifest Gitelman syndrome and impaired vasoconstriction. *J. Am. Soc. Nephrol.* **21,** 1868–1877
17. McCormick, J. A., Mutig, K., Nelson, J. H., Saritas, T., Hoorn, E. J., Yang, C. L., Rogers, S., Curry, J., Delpire, E., Bachmann, S., and Ellison, D. H. (2011) A SPAK isoform switch modulates renal salt transport and blood pressure. *Cell Metab.* **14,** 352–364
18. Grimm, P. R., Taneja, T. K., Liu, J., Coleman, R., Chen, Y. Y., Delpire, E., Wade, J. B., and Welling, P. A. (2012) SPAK isoforms and OSR1 regulate sodium-chloride co-transporters in a nephron-specific manner. *J. Biol. Chem.* **287,** 37673–37690
19. Filippi, B. M., de los Heros, P., Mehellou, Y., Navratilova, I., Gourlay, R., Deak, M., Plater, L., Toth, R., Zeqiraj, E., and Alessi, D. R. (2011) MO25 is a master regulator of SPAK/OSR1 and MST3/MST4/YSK1 protein kinases. *EMBO J.* **30,** 1730–1741
20. Gagnon, K. B., Rios, K., and Delpire, E. (2011) Functional insights into the activation mechanism of Ste20-related kinases. *Cell Physiol. Biochem.* **28,** 1219–1230
21. Ponce-Coria, J., Gagnon, K. B., and Delpire, E. (2012) Calcium-binding protein 39 facilitates molecular interaction between Ste20p proline alanine-rich kinase and oxidative stress response 1 monomers. *Am. J. Physiol. Cell Physiol.* **303,** C1198–C1205
22. Villa, F., Deak, M., Alessi, D. R., and van Aalten, D. M. (2008) Structure of the OSR1 kinase, a hypertension drug target. *Proteins* **73,** 1082–1087
23. Gagnon, K. B., and Delpire, E. (2010) Molecular determinants of hyperosmotically activated NKCC1-mediated K^+/K^+ exchange. *J. Physiol.* **588,** 3385–3396
24. Combs, S. A., Deluca, S. L., Deluca, S. H., Lemmon, G. H., Nannemann, D. P., Nguyen, E. D., Willis, J. R., Sheehan, J. H., and Meiler, J. (2013) Small-molecule ligand docking into comparative models with Rosetta. *Nat. Protoc.* **8,** 1277–1298
25. Wang, C., Bradley, P., and Baker, D. (2007) Protein-protein docking with backbone flexibility. *J. Mol. Biol.* **373,** 503–519
26. Alexander, N., Woetzel, N., and Meiler, J. (2011) in *IEEE 1st International Conference on Computational Advances in Bio and Medical Sciences* (*ICCABS*), *Orlando, FL, February 3–5, 2011*, pp. 13–18, Institute of Electrical and Electronics Engineers, Piscataway, NJ
27. Raveh, B., London, N., and Schueler-Furman, O. (2010) Sub-angstrom modeling of complexes between flexible peptides and globular proteins. *Proteins* **78,** 2029–2040
28. James, P., Halladay, J., and Craig, E. A. (1996) Genomic libraries and host strain designed for highly efficient two-hybrid selection in yeast. *Genetics* **144,** 1425–1436
29. Delpire, E., and Gagnon, K. B. (2008) SPAK and OSR1: STE20 kinases involved in the regulation of ion homoeostasis and volume control in mammalian cells. *Biochem. J.* **409,** 321–331
30. Gagnon, K. B., and Delpire, E. (2012) Molecular physiology of SPAK and OSR1: two Ste20-related protein kinases regulating ion transport. *Physiol. Rev.* **92,** 1577–1617
31. Kaufmann, K. W., Lemmon, G. H., Deluca, S. L., Sheehan, J. H., and Meiler, J. (2010) Practically useful: what the Rosetta protein modeling suite can do for you. *Biochemistry* **49,** 2987–2998
32. Milburn, C. C., Boudeau, J., Deak, M., Alessi, D. R., and van Aalten, D. M. (2004) Crystal structure of MO25α in complex with the C terminus of the pseudo kinase STE20-related adaptor. *Nat. Struct. Mol. Biol.* **11,** 193–200
33. Zeqiraj, E., Filippi, B. M., Deak, M., Alessi, D. R., and van Aalten, D. M. (2009) Structure of the LKB1-STRAD-MO25 complex reveals an allosteric mechanism of kinase activation. *Science* **326,** 1707–1711
34. Na, T., Wu, G., and Peng, J. B. (2012) Disease-causing mutations in the acidic motif of WNK4 impair the sensitivity of WNK4 kinase to calcium ions. *Biochem. Biophys. Res. Commun.* **419,** 293–298
35. Yang, C. L., Zhu, X., Wang, Z., Subramanya, A. R., and Ellison, D. H. (2005) Mechanisms of WNK1 and WNK4 interaction in the regulation of thiazide-sensitive NaCl cotransport. *J. Clin. Invest.* **115,** 1379–1387
36. Geng, Y., Hoke, A., and Delpire, E. (2009) The Ste20 kinases SPAK and OSR1 regulate NKCC1 function in sensory neurons. *J. Biol. Chem.* **284,** 14020–14028
37. Ahlstrom, R., and Yu, A. S. (2009) Characterization of the kinase activity of a WNK4 protein complex. *Am. J. Physiol. Renal Physiol.* **297,** F685–F692
38. Miyamoto, H., Matsushiro, A., and Nozaki, M. (1993) Molecular cloning of a novel mRNA sequence expressed in cleavage stage mouse embryos. *Mol. Reprod. Dev.* **34,** 1–7
39. Shin, J. H., Namkung, W., Choi, J. Y., Yoon, J. H., and Lee, M. G. (2004) Purinergic stimulation induces Ca^{2+}-dependent activation of Na^+-K^+-$2Cl^-$ cotransporter in human nasal epithelia. *J. Biol. Chem.* **279,** 18567–18574
40. Wilson, F. H., Disse-Nicodème, S., Choate, K. A., Ishikawa, K., Nelson-Williams, C., Desitter, I., Gunel, M., Milford, D. V., Lipkin, G. W., Achard, J. M., Feely, M. P., Dussol, B., Berland, Y., Unwin, R. J., Mayan, H., Simon, D. B., Farfel, Z., Jeunemaitre, X., and Lifton, R. P. (2001) Human hypertension caused by mutations in WNK kinases. *Science* **293,** 1107–1112
41. Boyden, L. M., Choi, M., Choate, K. A., Nelson-Williams, C. J., Farhi, A., Toka, H. R., Tikhonova, I. R., Bjornson, R., Mane, S. M., Colussi, G., Lebel, M., Gordon, R. D., Semmekrot, B. A., Poujol, A., Välimäki, M. J., De Ferrari, M. E., Sanjad, S. A., Gutkin, M., Karet, F. E., Tucci, J. R., Stockigt, J. R., Keppler-Noreuil, K. M., Porter, C. C., Anand, S. K., Whiteford, M. L., Davis, I. D., Dewar, S. B., Bettinelli, A., Fadrowski, J. J., Belsha, C. W., Hunley, T. E., Nelson, R. D., Trachtman, H., Cole, T. R., Pinsk, M., Bockenhauer, D., Shenoy, M., Vaidyanathan, P., Foreman, J. W., Rasoulpour, M., Thameem, F., Al-Shahrouri, H. Z., Radhakrishnan, J., Gharavi, A. G., Goilav, B., and Lifton, R. P. (2012) Mutations in kelch-like 3 and cullin 3 cause hypertension and electrolyte abnormalities. *Nature* **482,** 98–102
42. Ohta, A., Schumacher, F. R., Mehellou, Y., Johnson, C., Knebel, A., Macartney, T. J., Wood, N. T., Alessi, D. R., and Kurz, T. (2013) The CUL3-KLHL3 E3 ligase complex mutated in Gordon's hypertension syndrome interacts with and ubiquitylates WNK isoforms: disease-causing mutations in KLHL3 and WNK4 disrupt interaction. *Biochem. J.* **451,** 111–122
43. Wakabayashi, M., Mori, T., Isobe, K., Sohara, E., Susa, K., Araki, Y., Chiga, M., Kikuchi, E., Nomura, N., Mori, Y., Matsuo, H., Murata, T., Nomura, S., Asano, T., Kawaguchi, H., Nonoyama, S., Rai, T., Sasaki, S., and Uchida, S. (2013) Impaired KLHL3-mediated ubiquitination of WNK4 causes human hypertension. *Cell Rep.* **3,** 858–868